Characterization of Chip-Size Electrically-Small Antennas for Smart Wireless Biomedical Devices

H. Dinis, P. Anacleto, J. Fernandes, P. M. Mendes
Dept. of Industrial Electronics, University of Minho, Guimarães, Portugal

***Abstract* — The new requirements for smarter and smaller biomedical microsystems demand for new integration technologies, including antenna integration. This can be solved with the use of microfabrication technologies, allowing the fabrication of chip-size antennas that may be placed on top of silicon wafers. However, due to their ultra-small physical dimensions and special operating conditions (e.g., covered with body tissue phantoms), antenna characterization requires the use of auxiliary custom-made transitions between antenna and test equipment, which are much larger than the antennas under test. Since electrically small antennas show also very small gain, the use of test boards may carry a significant impact on the antenna's characteristics. This paper presents a methodology used to investigate the performance of chip-size 3D antennas (500x500x500 μm^3) designed to operate inside the human body in the frequency band 1-8 GHz.**

Keywords—microantenna integration; chip-size antennas; biomedical wireless system; antenna characterization.

I. INTRODUCTION

The miniaturization achieved by wireless devices (bellow the microscale) is driving their suitability to many new applications, being the biomedical field one of the most important. Neural implants [1], implantable chemical sensors [2], cardiac pacemakers, or cardioverter-defibrillators [3] are just a few examples of possible applications.

The use of microfabrication technologies [4, 5] allows for the fabrication of ultra-miniaturized microsystems with wireless communications and RF energy harvesting. However, to increase the degree of miniaturization, antennas should also be integrated with the final microdevice. Such integration solutions may allow the implementation of antenna on chip, or antenna in package. The most interesting solution for miniaturization is fabrication of ultra-small antennas using fabrication methodologies compatible with CMOS technology [6], which will allow the antennas to be placed on top of silicon wafers.

After fabrication of the ultraminiaturized antennas based on 3D self-folding methodologies for operation inside the human body, they need to be characterized. Although, the challenges we face are twofold. One is related with the antenna's ultra small size (in the present design, it should fit inside a cube no larger then 500x500x500 μm^3). The challenge arises from the need to connect such antenna to a 50 Ω connector, which is in the millimetre-centimetre scale. The other challenge is related with the body phantom cover placement. It is not difficult if we use a large amount of body phantom, which covers antenna and test board. However, when the phantom is required to have a volume slightly larger than the antenna, the radiation properties may change significantly with phantom volume.

Moreover, since we want to use a very small antenna to operate in the low gigahertz region (1-10 GHz), such antenna will be electrically small, with an efficiency that will be poor. That constitutes a problem since the radiation contribution from the test structure may turn to be not negligible, as happens for antennas with high radiation efficiency. In this way it may be difficult to understand what radiation is due to the antenna, and what is due to the test structure or body phantom itself. To avoid the issues associated with test boards, one characterization methodology that is many times adopted for ultra-small wireless links is to implement a setup that demonstrates the wireless link's ability to transmit the required power [7, 8]. Despite such methodology allowing for antenna indirect performance assessment, it gives few insights on antenna intrinsic operations properties. Also, it may not be easy to receive enough instantaneous power to light up a LED, mainly when we consider far-field solutions. Then, a methodology focused on antenna characterization should be implemented.

In this paper we present the methodology used to characterize the properties of highly integrated ultra-small small antennas. We propose a setup to characterize the antennas and we investigate the effects on radiation of the different elements involved in the measurement setup.

II. ANTENNA FABRICATION

The antenna under study is a 3D antenna fabricated using a self-folding fabrication technology [4]. Such technology was used to further increase the integration degree with RFCMOS circuitry, by placing antennas on top of silicon wafers (Fig. 1). Fig. 2 shows the fabrication steps required for the fabrication of such antenna, with interconnections, that remains on top of the wafer after the end of the processing steps.

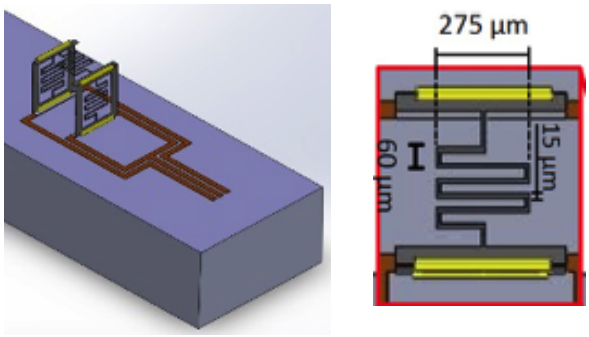

Fig. 1. Fabricated antenna (left), and detail on dimensions (right).

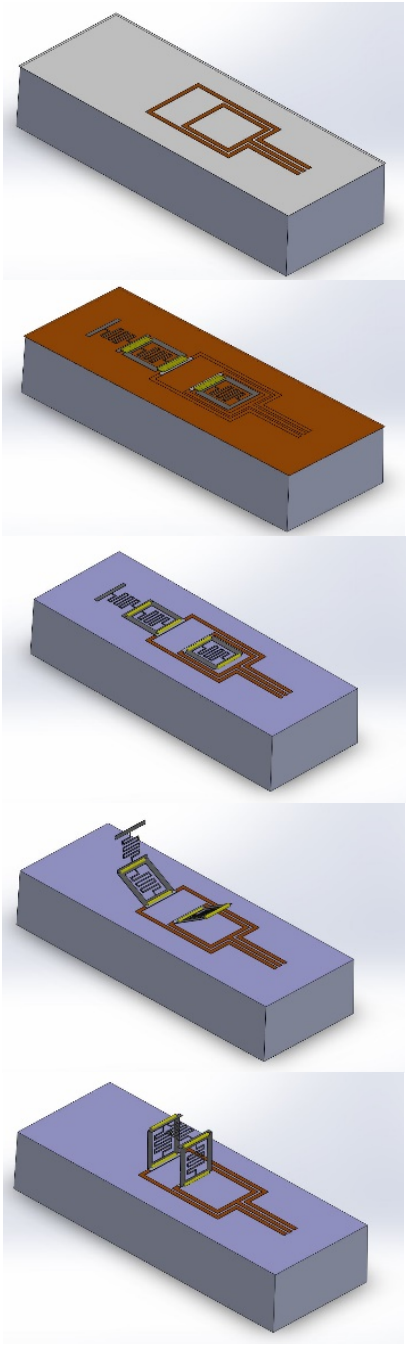

1- Clean Si wafer
2- Sputtering – Ta (10nm)
3- Sputtering – Cu (200nm)
4- Deposit – CuO (2µm)
5- Patterning – mask 1
6- Eletrodeposition – Cu (2µm)

7- Sputtering – Ta (10nm)
8- Sputtering – Cu (200nm)
9- Patterning – mask 2
10- Eletrodeposition – Ni (5µm)
11- Patterning – mask 3
12- Eletrodeposition – Tin (10µm)

13- Remove Cu seed layer
14- Remove Ta adhesion layer
15- Remove CuO
16- Remove Cu seed layer
17- Remove Ta adhesion layer

18- Increase temperature – Folding starts

19- Folding Complete

Fig. 2. Proposed fabrication methodology. Left side shows the schematic evolution of the antenna fabrication steps. Right side shows a brief description.

At the end of the fabrication steps, we arrive at a radiating structure that may be interfaced with a test board through the coplanar waveguide (CPW) feeding line. This solution is adequate for on-chip characterization using a RF probe station equipped with CPW probes. However, tests inside an anechoic chamber, to measure the radiation pattern, require the use of a RF PCB board between the final structure and an SMA connector.

III. Characterization Methodology

Since we require the test board for anechoic chamber characterization, and the test board may have influence in the antenna performance, different prototypes were considered for simulation and measurements.

A. Measurement Setup Modeling

As discussed previously, since the proposed antenna has an expected low efficiency (due to operation inside the lossy body tissues) and the transition structures are much larger than the antenna, it could be argued that such auxiliary structures are also, significantly, contributing for the overall radiation. To understand the behaviour of the auxiliary structures, different scenarios were modelled.

Since the interface between antenna and RF connector is much larger than the antenna itself, it is required to include the full interface in the HFSS model to properly assess the antenna performance. Fig. 3 shows the model built to include the antenna's, the body phantom, and the test board with a transition to the measurement instrument (coaxial to CPW with the ground plane shorted in one end).

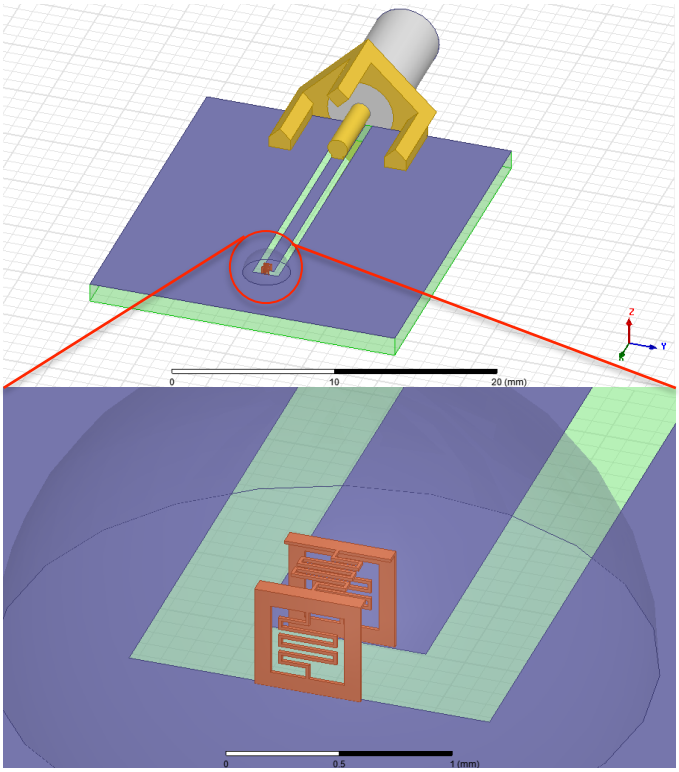

Fig. 3. HFSS model of test board with antenna and body phantom. Top part shows the full model, and the bottom shows a zoom-in in the antenna region. It can be observed a hemisphere on top of the antenna, which represents the body phantom volume. The antenna is designed on the surfaces of a 500x500x500 μm^3 cube.

Besides the model of Fig. 3, two other models were implemented to assess the antenna radiation effectiveness. One was the model of the test board itself, as shown in Fig. 4.

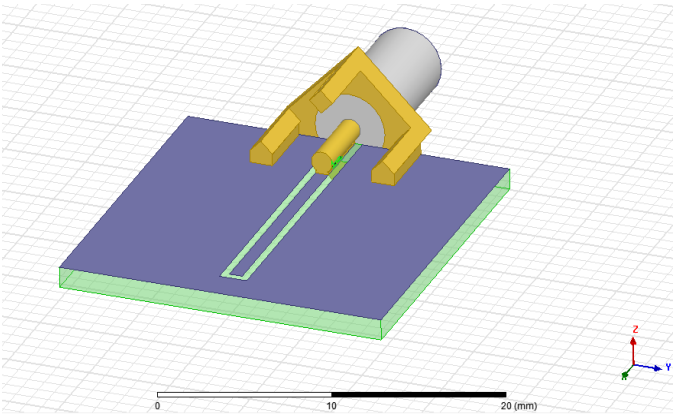

Fig. 4. HFSS model of test board, without antenna or body phantom.

The other model (Fig. 5) is the test board without the antenna but with the body phantom.

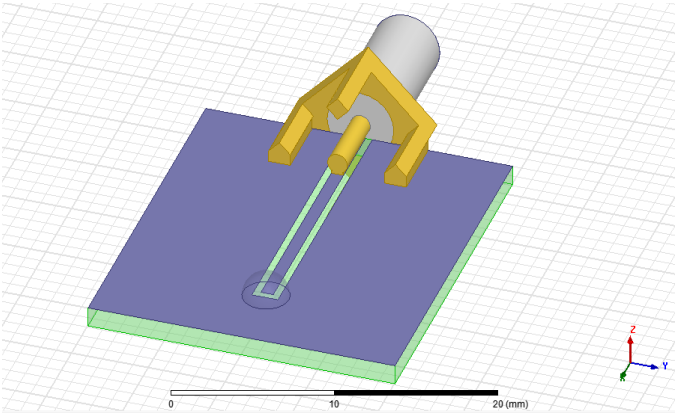

Fig. 5. HFSS model of test board with body phantom and without antenna.

The idea behind the decision of having these three models was to understand the radiation ability of each substructure that constitutes the full characterization setup.

B. *Measurement Setup Implementation*

For measurement purposes, the antennas were placed on top of test boards with dimensions and scenarios similar to the models shown previously. Fig. 6 shows a PCB board connected to a SMA connector in one end, where the other end is terminated in such a way that the antenna terminal may be placed between CPW ground plane and centre line.

After fabrication, and since it must operate inside the human body, the antenna must be characterized after being covered by body tissues that may be found in the operating scenarios. The solution for this need can be observed in the foreground image in Fig. 6. It can be observed that the antenna is surrounded by nail polish to allow body phantom enclosure around the antenna. The microantenna was mounted on different board sizes and CPW line configurations (keeping the line impedance at 50 Ω), to understand if different interface boards would have a different impact on antenna performance. It was also possible modify the body phantom to: tap water, DI water, salt water, and alcohol. This paper will discuss only results based on tap water.

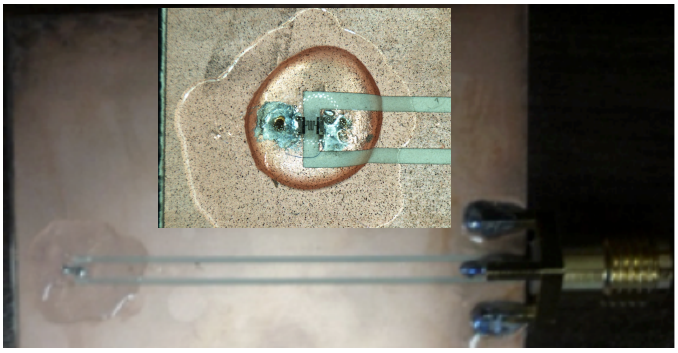

Fig. 6. Fabricated antenna mounted on test structure. The background image shows the full board, and the foreground shows a zoom in of the antenna, placed at the end of the CPW feed line.

Since the radiation properties associated wit the CPW line itself will depend on the length of such line, different boards with different lengths (under the conditions of Fig. 3, Fig. 4, and Fig. 5) were tested. After a few measurements of S11, the board with a length of 20 mm was selected for antenna pattern measurements, since that board, while in the scenario of Fig. 4, shows a S11 where no power is being fed into the structure in the antenna's operating frequency.

IV. Results and Discussion

The proposed scenarios were simulated, measured, and compared to find a modelling approach that would allow a correct prediction of antenna performance.

A. *Measurement Setup*

Fig. 7 shows the setup used for test board characterization. The measurements were accomplished inside an anechoic chamber.

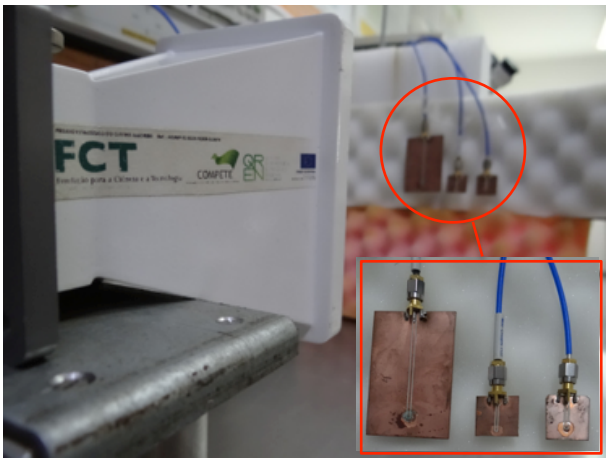

Fig. 7. Test setup to measure the different test boards (with and without antenna, with and without body phantoms).

As a standard gain antenna, the broadband horn antenna (Q-par Angus, Ltd. WBH2-18S) was used. This will limit our tests to 2-18 GHz, which is not a problem.

B. *S11 Parameter Assessment*

From the different possible body phantom like materials, the next results were obtained using tap water. Fig. 8 shows the

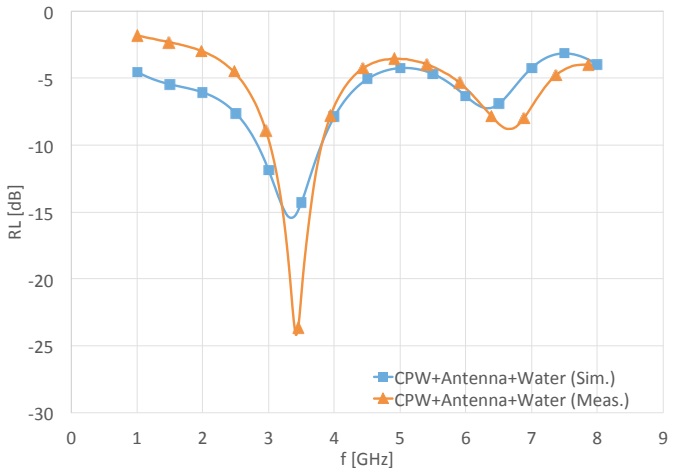

Fig. 8. S11 parameter for CPW loaded with antenna and body phantom (tap water - cf. Fig. 2).

S11 parameters when the test board includes the microantenna covered by the body phantom. It can be observed a good agreement between measured and simulated results, as well that the antenna operating frequency is 3.4 GHz.

Fig. 9 shows the results when the test board is loaded only with water at the feeding point.

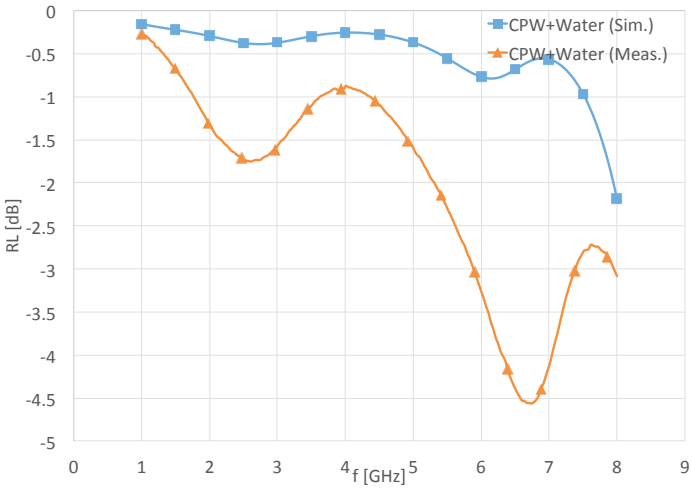

Fig. 9. S11 parameter for CPW loaded with body phantom (tap water – cf. Fig. 4).

Again, an acceptable agreement between measurements and simulations can be observed. The peak at 3.4 GHz disappeared, which means that the microantenna has an influence in the overall operation characteristics of the test board.

Fig. 10 shows the data when only the antenna is placed on top of the test board. Again, a good agreement was registered between measurements and simulations. And, again, no peak at 3.4 GHz was observed. From the previous results we conclude that the characterization of S11 is a relatively easy task and the measured values shows good agreement with the simulations. However, repeatability for different measurements under the same scenario was not a trivial task. One problem was the ability to repeat the size of the water drop on top of the

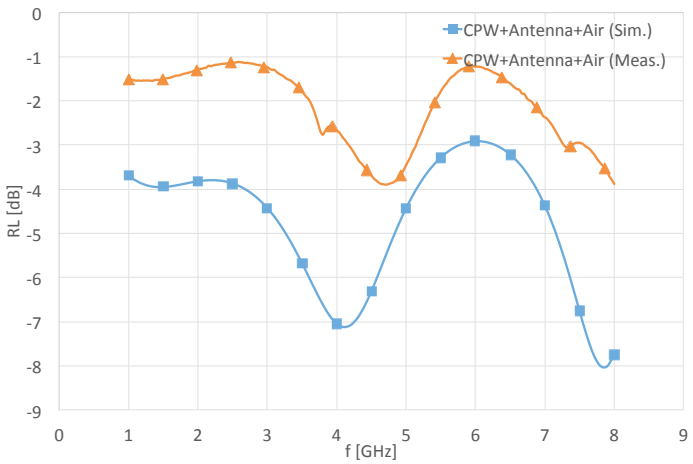

Fig. 10. S11 parameter for CPW loaded with antenna.

antenna while the other issue was the evaporation of the phantom. This issue is being addressed and the new prototypes should handle it using a PDMS microbox placed around the antenna.

C. Radiation Pattern Assessment

The next step was to characterize the radiation pattern and to obtain the antenna gain.

Fig. 11 shows the gain radiation patterns for the test board only and loaded with the microantenna, and without any phantom (S11 in Fig. 10).

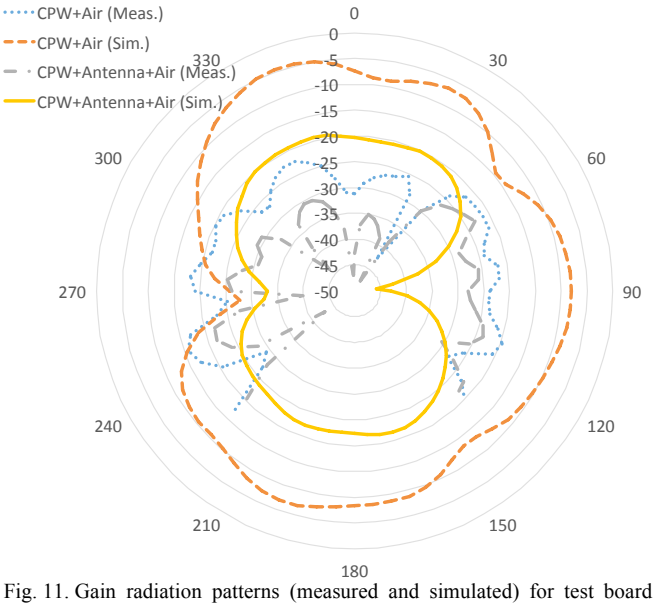

Fig. 11. Gain radiation patterns (measured and simulated) for test board not loaded and loaded only with the antenna, at 3.4 GHz in the azimuth plane.

The main conclusion that be extracted from Fig. 11 is that simulated and measured results barely agree.

Fig. 12 shows the scenario where the test board is loaded with water (phantom), and with antenna and water. Again, it can be observed that the simulated patterns significantly differ from the measured ones. The positive aspect that can be observed is the tendency observed for the measurement, where the highest gain occurs for the scenario when we have the test

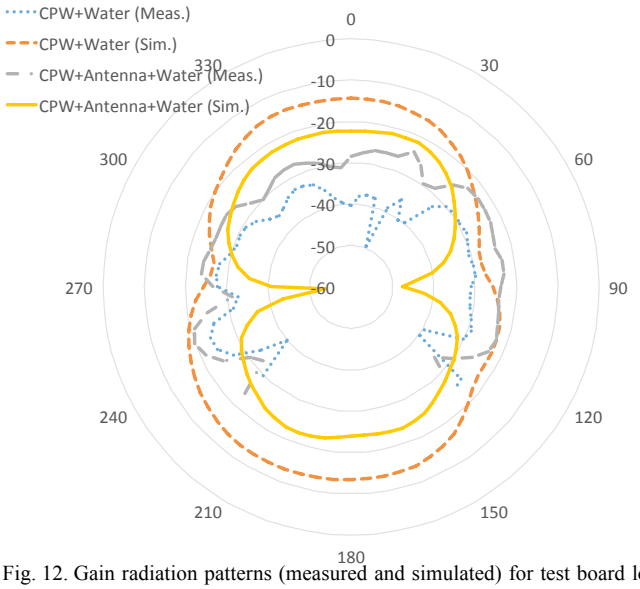

Fig. 12. Gain radiation patterns (measured and simulated) for test board loaded with water and with water and with antenna, at 3.4 GHz in the azimuth plane.

board loaded with antenna and phantom, which is the desired operating scenario.

However, when we compare Fig. 11 and Fig. 12, it is possible to observe that the scenario were radiation should occur shows a gain in the same order of the gain for scenarios were no radiation should occur. This is due to the fact that the proposed antennas are electrically very small, leading to very small efficiencies.

V. Conclusions

This paper discusses testing of ultra-small and electrically-small antennas. It was verified that the proposed methodology was useful to obtain the power transfer characteristic for the proposed antennas. For such antennas it was possible to predict the S11 parameters from HFSS simulations, however, the gain radiation pattern was very difficult to predict.

So far, the methodology was used to conclude that the chip-size ultra-small antennas, despite their low efficiency, are operating as radiators. However, more effort should be placed on the experimental side to improve the measured results. Such efforts must be able to reduce the effect of the radiation from the test boards, which should not be neglected for this antenna size and operating conditions. Moreover, the design should be improved to allow an easy reproduction of measured results when the body phantom is used.

Acknowledgment

This work was supported by Portuguese Foundation for Science and Technology: FCT-PTDC/EEI-TEL/2881/2012, Programa Operacional Temático Fatores de Competitividade (COMPETE) and Fundo Comunitário Europeu FEDER.

References

[1] - K. Wise, D. Anderson, J. F. Hetke, D. Kipke, and K. Najafi, “Wireless implantable microsystems: high-density electronic interfaces to the nervous system,” Proc. IEEE, vol. 92, no. 1, pp. 76–97, Jan. 2004.

[2] - M. C. Frost and M. E. Meyerhoff, “Implantable chemical sensors for real-time clinical monitoring: progress and challenges,” Curr. Opin. Chem. Biol., vol. 6, no. 5, pp. 633–641, 2002.

[3] - M. Rasouli and L. S. J. Phee, “Energy sources and their development for application in medical devices,” Expert Rev. Med. Devices, vol. 7, no. 5, pp. 693–709, 2010.

[4] - C. L. Randall, E. Gultepe, and D. H. Gracias, “Self-folding devices and materials for biomedical applications,” Trends in Biotechnology, vol. 30, no. 3. pp. 138–146, 2012.

[5] - K. Kurselis, R. Kiyan, V. Bagratashvili, V. K. Popov, B. N. Chichkov, “3D fabrication of all-polymer conductive microstructures by two photon polymerization,” Opt. Express, vol. 21, no. 25, p. 31029, 2013.

[6] - S. Gomes, J. Fernandes, P. Anacleto, E. Gultepe, D. Gracias, P. M. Mendes, “Ultra-Small Energy Harvesting Microsystem for Biomedical Applications,” in 44st European Microwave Conference (EuMC), 2014.

[7] – A. S. Y. Poon, S. O’Driscoll, and T. H. Meng, “Optimal frequency for wireless power transmission into dispersive tissue,” IEEE Trans. Antennas and Propagation, 58, 1739, 2010.

[8] - J. S. Ho, A. J. Yeh, E. Neofytou, S. Kim, Y. Tanabe, B. Patlolla, R. E. Beygui, and A. S. Y. Poon, “Wireless power transfer to deep-tissue microimplants,” PNAS, 111, 7974-7979 (2014)